2021 6th International Conference for Convergence in Technology (I2CT)
Pune, India. Apr 02-04, 2021

Local Quality Pattern (LQP) : A Quality Aware Local Statistical Feature Descriptor for No-Reference Image Quality Assessment

Chirag Kyal, Harsh Poddar
National Institute of Science and Technology
Berhampur, India
chirag.kyal@gmail.com, harshpoddar1549@gmail.com

Shubhobrata Bhattacharya
Indian Institute of Technology Kharagpur
Kharagpur, India
emailshubho@gmail.com

2021 6th International Conference for Convergence in Technology (I2CT) | 978-1-7281-8876-8/21/$31.00 ©2021 IEEE | DOI: 10.1109/I2CT51068.2021.9418050

***Abstract*—Assessment of the quality of the no-reference images in real-life applications is of immense importance. The no-reference image quality assessment (NR-IQA) algorithms are designed to measure quantitatively and accurately the perpetual quality of an image without any prior knowledge about its reference. In this work, we have proposed a novel NR-IQA metric to replicate the human visual system (HVS) for the perception of image distortion using the structural details and luminance information of the image. We propose a local descriptor that extracts the perceptual structural features of the image with highlighted reflectance to represent the variation of illuminance in the distorted probe image. We name this quality-aware descriptor as Local Quality Pattern (LQP). The extracted features are trained with support vector regression (SVR) to model the mapping of the feature vectors with the quality measure. Finally, the metric obtained is named Local Quality Pattern Score (LQPS). Extensive experiments conducted on publicly available datasets namely, LIVE, MLIVE and CSIQ databases to show that the proposed LQPS metric outperforms the compared NR-IQA methods with a prominent margin.**

***Index Terms*—No-reference image quality, Lambertian Reflection Model, Hashing, Support Vector Regression (SVR).**

I. Introduction

The advent of sensor technology and communication technologies, taking photos and sharing on different multimedia platforms has become a part of our quotidian existence. However, the digital images captured from different sources (sensors) are often subjected to variety of distortions during acquisition, compression, transmission, and reproduction. These necessities the need for the proper estimation of visual quality before any further processing and presentation to the end-viewer. Hence image quality assessment (IQA) has become an undeniable part of multimedia applications.

Based on the availability of reference images, image quality assessment (IQA) is categorized into three classes : Fully Reference (FR), Reduced Reference (RR) and No Reference (NR) metrics. Among these three categories, the NR-IQA is the most challenging, due to the unavailability of the reference images. Hence NR-IQA gets more important for further research. Most of the NR-IQA algorithms rely on the same framework of extracting the features from the images and estimate the quality score base on the pre-trained model. Hence it can be said that the extracted features play a key role in projecting the type and degree of distortion in the image. The literature survey suggests, there are two categories on which the feature extraction techniques of IQA can be classed : natural scene statistic (NSS)-based approaches and learning-based approaches [1], [2], [3]. NSS-based approaches are based on certain statistical properties which can be presented using statistical models like Gaussian distributions along with properties of cosines [4], contourlet coefficients [5] and wavelets [6]. The variation of the parameters of the model depends on the degree of distortion introduced in the training image sets. The learning-based approach relies on the extracted features from the training image set which are then trained with the regression models like Random Forest (RF), Support Vector Regression (SVR) etc. for mapping the score of a probe image based on similar features. In most of the state-of-the-art (SOA) methods experiment has been done on images with single distortion (in most of the cases the distortions are artificially imposed on the images). However in real world scenario the acquisition of images undergoes multiple distortions such as blur, noise, illumination etc [7]. Hence there is a need to develope a NR-IQA method which can address scenario of multiple distortions of the probe image as it is more meaningful for real life purposes.

Some of the prominent working on NR-IQA like [8] relied on local binary pattern (LBP) or its variants for quality assessment. LBP is a binary encoding based representation of the image structure and it gives a gross approximation of human visual system (HVS). The LBP operator binarize the pixel to pixel relation by thresholding (either 0s or 1s) the difference of intensity of neighborhood of each pixel with the center pixel value. However, the performance of LBP is not adequate to capture the local structural details due to it lacks magnitude information. In other words, the thresholding operation of LBP marginalizes the pixel to pixel information and hence cannot give a suitable representation for HVS. Hence, there is still considerable scope for improvement. In [9], Wang et. al

978-1-7281-8876-8/21/$31.00 ©2021 IEEE

proposed an NR-IQA method for JPEG compressed images by calculating between-block differences in the spatial domain. In [10], the quality of blurred images is obtained with an average spread of the structural edges. In the works of [11], the image quality due to compression is measured using pixel distortions and edge features. Image contrast distortion is used for quality estimation using statistical descriptors of image luminance in [12]. However, since these are distortion-specific NR-IQA methods, their practical usage of multi-distortion applications is limited. In this paper we propose a novel no reference image quality metric for multiple distortions, based on quality aware feature descriptor. The contribution of the work is two folded. Firstly, we proposed a quality aware feature descriptor to replicate the human visual mechanism. The descriptor captures local stuctural details of the image and encodes them into a histogram feature vector. Unlike the features obtained from LBP, Gabor, LDP etc, the proposed feature is more sensitive to the changes due to the presence of factors like JPEG2000 (JP2K) compression, Gaussian blur (GB), Gaussian white noise (WN) and contrast change. The proposed descriptor is named as Local Quality Pattern (LQP) based on the nature of its performance. The LQP encode the microstructure of the images based on image reflectance model which is more susceptable to human vision. Next, the histogram feature of the transformed image of LQP is trained with the SVR model. Experiments were conducted on publicly available databases to demonstrate the performance of the proposed method.

The remaining paper is organized as follows. LQP is explained in Section II. The section also includes the description of training the LQP features using SVR. The results of the experiments conducted is presented in Section III. The conclusion is given in Section V.

II. Proposed Method

In the proposed work, we have attempted to imitate the early vision stage using a statistical model along with a representative local structure feature that is affected by quality variation. The quality-aware descriptor feature is named Local Quality Pattern (LQP). The formulation of LQP is based on three subsections i.e, (a) Reflectance part of the image is highlighted with LRM; (b) Calculation of Logarithmic Pixel Difference Vector (LPDV); (c) Logarithmic Pixel Difference Vector Hash (LPDVH) encoding, and (d) Feature extraction. The obtained feature is used to train the Support Vector Regressor (SVR) model for the assessment of the quality of distorted natural images. In the following section, we have explained these steps in details.

A. Lambertian Reflectance Model (LRM)

The pixel to pixel relation has been successfully used in multiple applications of image processing, texture recognition, face recognition, etc. In all these cases pixel to pixel relation is used by exploiting different interaction between the central pixel and its neighbors in a window. To understand the pixel-to-pixel charecteristics of an image, we first discuss Lambertian Reflectance Model (LRM). By LRM any pixel of an image can be represented as a product of reflectance (G) and luminance (L). Hence an image can be represented as $I(x,y) = G(x,y).L(x,y)$, where $I(x,y)$ is the pixel intensity at position (x,y). L is the low frequency component of the image and experience slow variations even when there are abrupt changes in G. This property is stated as $L(x \pm \Delta x, y) \simeq L(x, y \pm \Delta y) \simeq L(x \pm \Delta x, y \pm \Delta y) \simeq L(x,y)$ where $\pm\Delta x$ and $\pm\Delta y$ denotes small changes in pixel position in all directions (denoted by $\pm$ symbol). The illustration in Fig. 1 explains the concept in details. In [13], Chen et al exploited these relations of LRM by the quotient operation of (1). By this relation, the luminance portion of the image intensity is nullified and the reflectance characteristics is highlighted in the image. This theory finds a successful application in the work of [13] for face recognition.

$$W(x,y) \simeq \arctan\left[\zeta \sum_{i\in A}\sum_{j\in A} \frac{I(x,y) - I(x+i\Delta x, y+j\Delta y)}{I(x,y)}\right] \simeq \arctan\left[\zeta \sum_{i\in A}\sum_{j\in A} \frac{G(x,y) - G(x+i\Delta x, y+j\Delta y)}{G(x,y)}\right] \quad (1)$$

where $A \in \{-1, 0, +1\}$. In (1), ζ is a weighting parameter, whose weight is optimally taken as 4 by [13]. The relation of (1) is relevantly applied to many applications of face recognition [14], [15], [16], [17], [18], [19], [16]. Although the relation (1) gives promising result in giving face representation, with luminance effect nullified, it has some challenges in numerical calculations. When the denominator is close to zero and the numerator is large, the quotient can be arbitrarily large, which may excessively amplify the difference between the numerator and denominator. Some quotient based model like [14] uses a regularization term in the denominator to relieve the problem. Other methods [16], [17] uses modified version of the quotient relation (1) to avoid the denominator related problems. Another problem of relation (1) is that, with the increase in size of the window i.e, increase in the number of participating pixels, the relaxation becomes ineffective.

$\tilde{G}(x-\Delta x, y+\Delta y)+\tilde{L}(x,y)$	$\tilde{G}(x, y+\Delta y)+\tilde{L}(x,y)$	$\tilde{G}(x+\Delta x, y+\Delta y)+\tilde{L}(x,y)$
$\tilde{G}(x-\Delta x, y)+\tilde{L}(x,y)$	$\tilde{G}(x, y)+\tilde{L}(x,y)$	$\tilde{G}(x+\Delta x, y)+\tilde{L}(x,y)$
$\tilde{G}(x-\Delta x, y-\Delta y)+\tilde{L}(x,y)$	$\tilde{G}(x, y-\Delta y)+\tilde{L}(x,y)$	$\tilde{G}(x+\Delta x, y-\Delta y)+\tilde{L}(x,y)$

(a)

$\tilde{G}(x-\Delta x, y+\Delta y)-\tilde{G}(x,y)$	$\tilde{G}(x, y+\Delta y)-\tilde{G}(x,y)$	$\tilde{G}(x+\Delta x, y+\Delta y)-\tilde{G}(x,y)$
$\tilde{G}(x-\Delta x, y)-\tilde{G}(x,y)$		$\tilde{G}(x+\Delta x, y)-\tilde{G}(x,y)$
$\tilde{G}(x-\Delta x, y-\Delta y)-\tilde{G}(x,y)$	$\tilde{G}(x, y-\Delta y)-\tilde{G}(x,y)$	$\tilde{G}(x+\Delta x, y-\Delta y)-\tilde{G}(x,y)$

(b)

Fig. 1: The diagram demonstrates the difference operation of the central pixel from its neighbouring pixels to obtain the LPDV. The same operation is repeated with other pixel positions as shown in Fig. (2).

B. Logarithm Pixel Difference Vector (LPDV)

The Logarithmic Pixel Difference Vector (LPDV) is obtained by computing the difference among all the central

pixel and the peripheral pixels of the window. We define the window as $\eta_{(x_c,y_c)}$ such that $\eta_{(x,y)} \triangleq \{1 \leq |x_c - x_{n_i}| \leq R$ and $1 \leq |y_c - y_{n_i}| \leq R\}$. Here (x_c, y_c) and (x_{n_i}, y_{n_i}) denotes the central and peripheral pixels respectively and i ranges from 1 to $8R$. R is the radius of the filter ie, the step length between (x_c, y_c) and (x_{n_i}, y_{n_i}). For a window of size $[(2R+1)\times(2R+1)]$ the number of LPDV obtained is of length $L = 8R$ values. The difference of logarithm of pixels nullifies the effect of luminance and only retains the reflectance portion of the image. Logarithm converts multiplication of LRM into an additive model :

$$\tilde{I}(x,y) = \log_2[I(x,y)] = \log_2[G(x,y)] + \log_2[L(x,y)] \quad (2)$$

The assumption of the relations in LRM (section II-A) can be extended in relation (2) to get

$$\begin{aligned} &| \tilde{I}(x_1,y_1) - \tilde{I}(x_2,y_2) | = \\ &| \log_2[G(x_1,y_1)] - \log_2[G(x_2,y_2)]\} + \\ &\{\log_2[L(x_1,y_1)] - \log_2[L(x_2,y_2)] | \\ &\approx | \log_2[G(x_1,y_1)] - \log_2[G(x_2,y_2)] | \end{aligned} \quad (3)$$

where (x_1, y_1) and (x_2, y_2) are two pixel positions with in $\eta_{(x_c,y_c)}$. The operation is shown in the Fig. 2 and Fig. 1 . The LPDVs obtained from each pixel are further processed to obtain quality sensitive features which is discussed in upcoming sections. Logarithm differences $| \tilde{I}(x_1,y_1) - \tilde{I}(x_2,y_2) |$ are elements to emphasize the reflectance of the image. They are devoid of the challenges due to quotient models. It also reflects the difference between two pixels properly.

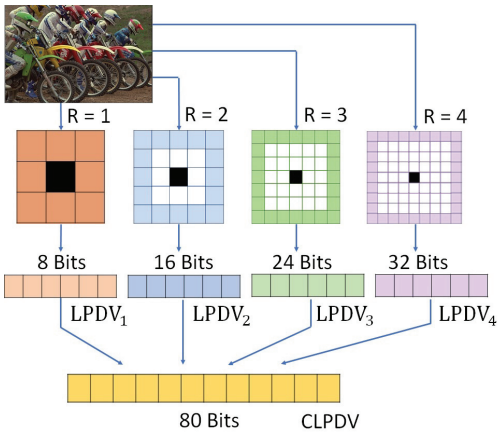

Fig. 2: The diagram shows the relation among the combination of pixels in the window of the descriptor

C. Logarithmic Pixel Difference Hashing (LPDH)

LPDV obtained from each window are concatenated to form the complete logarithmic pixel difference vector (CLPDV). We consider up to four windows of LQP (i.e, $R_m = 4$) for our experiment.Here R_m is the maximum radius of the window considered by LQP. Hence the length of CLPDV is $N = 4[R_m(R_m + 1)]$. For $R_m = 4$ the value of N is 80. The CLPDV is projected on to the hash dictionary formed using ITQ to obtain an 8 bit binary string. This binary string is converted to a decimal value and used as the encoded pixel i,e. the obtained scalar value replaces the central pixel of the designated window. The detail of ITQ is discussed in [20]. The projection operation is shown schematically in Fig. (3). With the increase in R_m, the bit length of CLPDV i.e N increases and hence the dictionary size also grows. However, the projected array of LPDV is binary and always 8 bit. The size of the codebook is $(N \times 8)$. The histogram of the transformed images is named as LPDH features and designated as (λ) for further analysis. The LPDH features are sensitive to the changes in heterogeneous image quality.

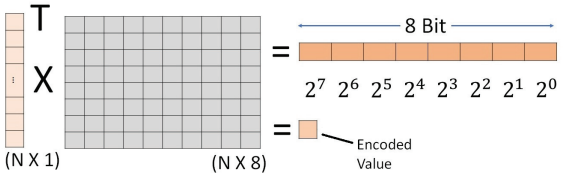

Fig. 3: The diagram represents the projection of CLPDV on the hashed ITQ dictionary to obtain an 8-bit binary string and the final encoded pixel

D. Local Quality Pattern Score (LQPS)

To predict the score of the image from the LPQ feature vector (λ), we used a trained SVR model. The use of SVR is prevalent in other NR-IQA algorithms like [21], [22] etc. Hence we have reliably used the same approach in our work. Moreover, SVR performs well with the features of higher dimensions [23]. We trained the SVR model with the subjective scores provided with the databases.

$$Q = SVR(\lambda, \mathcal{M}), \quad (4)$$

Here $\mathcal{M}$ denotes the trained model for regression and Q denotes the score predicted using the model.

III. Experimental Setup

The experiment for evaluation of the proposed LQPS method is done using three well-accepted public databases. The first database is the LIVE IQA database [24] which includes 29 reference images and 779 distorted images. The images are corrupted by five types of distortions: JPEG2000 compression (JP2K), JPEG, Gaussian white noise (WN), Gaussian blur (GB), and fast fading (FF). Subjective quality scores are provided as difference mean opinion score (DMOS) (range 0 to 100). The second is the CSIQ database [25]. It comprises 30 reference images and 866 distorted images. The images are perturbed by six types of distortions: JPEG, JP2K, WN, GB, Gaussian noise (GN), and contrast decrements (CTD). Subjective quality scores are provided in the form of DMOS ranging from 0 to 1. The third database is MLIVE, an extension of the LIVE database with multiple distortions. The database contains 15 reference images and 450 distorted

TABLE I: Performance comparison of LIVE Image database for different state-of-the-art methods

	SRCC	PLCC	RMSE
PSNR [27]	0.874	0.883	12.788
SSIM [27]	0.941	0.937	9.742
NIQE [3]	0.911	0.910	11.419
BIQI [6]	0.819	0.842	15.024
DIIVINE [21]	0.917	0.921	12.029
BLIINDS2 [4]	0.927	0.929	9.476
CORNIA [26]	0.937	0.954	9.167
BRISQUE [1]	0.946	0.951	8.974
NR-GLBP [26]	0.941	0.947	9.103
NFERM [2]	0.940	0.941	9.112
NRSL [8]	0.952	0.956	8.018
LQPS	**0.963**	**0.958**	**7.894**

TABLE II: Performance comparison of CSIQ Image database for different state-of-the-art methods

	SRCC	PLCC	RMSE
PSNR [27]	0.931	0.849	0.143
SSIM [27]	0.926	0.931	0.110
NIQE [3]	0.878	0.891	0.122
BIQI [6]	0.819	0.870	0.135
DIIVINE [21]	0.881	0.912	0.121
BLIINDS2 [4]	0.906	0.941	0.101
CORNIA [26]	0.891	0.927	0.103
BRISQUE [1]	0.903	0.937	0.101
NR-GLBP [26]	0.924	0.952	0.098
NFERM [2]	0.930	0.952	0.081
NRSL [8]	0.930	0.954	0.084
LQPS	**0.935**	**0.958**	**0.084**

images. Images are distorted with GB+JPEG and GB+WN. DMOS ranging from 0 to 100 is provided in the database. The proposed approach required training in two folded way. Firstly the codebook for encoding the PDV is needed to trained and secondly, the SVR is needed to be trained for proper assessment of the quality score. Hence to train the LQP and SVR we split the LIVE database into eighty percent training and twenty percent testing non-overlapping subset. The performance of IQA algorithms is evaluated by three different metrics: Spearman rank-order correlation coefficient (SRCC) to measure prediction monotonicity, Pearson linear correlation coefficient (PLCC) to measure prediction accuracy and root mean squared error (RMSE) to measure prediction error. Proposed LQPS is compared with the SOA NR-IQA methods, which includes NIQE [3], BIQI [6], DIIVINE [21], BLIINDS2 [4], CORNIA [22], BRISQUE [1], NR-GLBP [26], NFERM [2] and NRSL [8]. We also used PSNR and SSIM [27] for evaluation of LQP.

IV. Results and Discussion

The prediction performance measured by SROCC, PLCC, and RMSE values for three datasets is shown in Table I, II, and III. The results show the superiority of the proposed metric over the existing matrices as they are marked in bold in the table.

We further have shown the prediction score of SROCC for individual distortions in each database. For the LIVE database, we find in the experiment that the proposed method

TABLE III: Performance comparison of MLIVE Image database for different state-of-the-art methods

	SRCC	PLCC	RMSE
PSNR [27]	0.732	0.815	10.934
SSIM [27]	0.901	0.927	6.970
NIQE [3]	0.793	0.860	9.437
BIQI [6]	0.883	0.905	7.833
DIIVINE [21]	0.866	0.898	8.257
BLIINDS2 [4]	0.886	0.903	8.125
CORNIA [26]	0.900	0.915	7.586
BRISQUE [1]	0.901	0.924	7.275
NR-GLBP [26]	0.892	0.904	7.936
NFERM [2]	0.899	0.919	7.413
NRSL [8]	0.932	0.946	5.943
LQPS	**0.943**	**0.951**	**5.367**

outperforms the compared methods in the test for individual distortions. This is depicted in Table. IV. The table shows for WN, the SROCC score is better than LQPS by a narrow margin of 0.004 for PSNR and NRSL methods. Similarly, for FF distortion the score of LQPS is at per with the score of CORNIA. However, the overall score of LQPS for the whole LIVE database is superior to the state-of-the-art as shown in table I. Similarly, for the CSIQ database, the SROCC for individual distortions are reported in Table V. For JPEG compression the SRCC score of SSIM is found to be slightly higher than the proposed metric and for GB the SRCC score is similar to LQPS as reported in the table. However, the overall prediction score for the CSIQ database is found to be better than state of the art methods as shown in Table II. MLIVE database is more challenging due to multiple distortions. The experiment shows the superiority of the proposed work over the existing methods in Table VI a hence proves its superiority.

V. Conclusion

In this work, an NR-IQA algorithm is proposed namely LQP. The LQP features rely on local structural details and luminance base information of the image. In most of the NR-IQA methods, features are obtained from transformed image coefficients with a specific probability distribution to estimate the quality score. However, we have proposed a local descriptor that captures the structural details of the image and utilizes a statistical distribution to normalize the illumination map and replicate HVS as close as possible. The feature extracted in the due process is more quality-aware than most of the descriptor features in use. The illuminance normalization portion of the descriptor nullifies the effects of luminance and highlighting the reflectance representation of the image. The coding part of the descriptor encodes the inter-pixel relationship patterns which are prone to various distortions. Our findings in this work suggest that the complementary information on structural and illuminance can be a better feature representation for the quality assessment task. Extensive experiments with three widely used IQA public databases have been done. The results demonstrate that the proposed method LQPS is more competent than the compared methods. As future work, we would like to extend the application of LQPS to other arenas of

TABLE IV: SRCC comparison of LQP with different SOA methods for LIVE Image database.

Distortion	PSNR	SSIM	NIQE	BIQI	DIIVINE	BLIINDS2	CORNIA	BRISQUE	NR-GLBP	NFERM	NRSL	LQPS
JP2K	0.903	0.959	0.923	0.780	0.902	0.928	0.922	0.915	0.933	0.937	0.943	**0.945**
JPEG	0.891	0.975	0.942	0.829	0.899	0.949	0.941	0.963	0.958	0.964	0.960	**0.964**
WN	**0.984**	0.976	0.972	0.958	0.981	0.945	0.963	0.978	0.981	0.981	**0.984**	0.980
GB	0.808	0.960	0.941	0.844	0.935	0.913	0.955	0.946	0.936	0.909	0.959	**0.964**
FF	0.895	0.885	0.862	0.739	0.858	0.873	**0.910**	0.887	0.853	0.850	0.880	**0.910**

TABLE V: SRCC comparison of LQP for different SOA methods for CSQI Image database.

Distortion	PSNR	SSIM	NIQE	BIQI	DIIVINE	BLIINDS2	CORNIA	BRISQUE	NR-GLBP	NFERM	NRSL	LQPS
JP2K	0.942	0.970	0.927	0.815	0.877	0.889	0.901	0.892	0.911	0.917	0.921	**0.938**
JPEG	0.902	**0.957**	0.883	0.856	0.887	0.916	0.886	0.918	0.926	0.927	0.936	0.943
WN	0.940	0.823	0.837	0.842	0.901	0.899	0.797	0.919	0.925	0.934	0.955	**0.968**
GB	0.935	**0.937**	0.906	0.837	0.898	0.919	0.907	0.913	0.921	0.924	0.926	**0.937**

TABLE VI: SRCC comparison of LQP for different SOA methods for MLIVE Image database.

Distortion	PSNR	SSIM	NIQE	BIQI	DIIVINE	BLIINDS2	CORNIA	BRISQUE	NR-GLBP	NFERM	NRSL	LQPS
GB+JPEG	0.736	0.898	0.899	0.881	0.864	0.892	0.904	0.905	0.897	0.919	0.928	**0.931**
GB+WN	0.743	0.912	0.833	0.883	0.877	0.884	0.900	0.900	0.905	0.887	0.937	**0.942**

quality based applications like face quality assessment (FQA), hyperspectral image quality assessment (HSI-IQA), etc.

REFERENCES

[1] A. Mittal, A. K. Moorthy, and A. C. Bovik, "No-reference image quality assessment in the spatial domain," *IEEE Transactions on image processing*, vol. 21, no. 12, pp. 4695–4708, 2012.

[2] K. Gu, G. Zhai, X. Yang, and W. Zhang, "Using free energy principle for blind image quality assessment," *IEEE Transactions on Multimedia*, vol. 17, no. 1, pp. 50–63, 2014.

[3] A. Mittal, R. Soundararajan, and A. C. Bovik, "Making a "completely blind" image quality analyzer," *IEEE Signal Processing Letters*, vol. 20, no. 3, pp. 209–212, 2012.

[4] M. A. Saad, A. C. Bovik, and C. Charrier, "Blind image quality assessment: A natural scene statistics approach in the dct domain," *IEEE transactions on Image Processing*, vol. 21, no. 8, pp. 3339–3352, 2012.

[5] W. Lu, K. Zeng, D. Tao, Y. Yuan, and X. Gao, "No-reference image quality assessment in contourlet domain," *Neurocomputing*, vol. 73, no. 4-6, pp. 784–794, 2010.

[6] A. K. Moorthy and A. C. Bovik, "A two-step framework for constructing blind image quality indices," *IEEE Signal processing letters*, vol. 17, no. 5, pp. 513–516, 2010.

[7] S. Bhattacharya and A. Routray, "Score based face quality assessment (fqa)," in *2017 14th IEEE India Council International Conference (INDICON)*. IEEE, 2017, pp. 1–6.

[8] Q. Li, W. Lin, J. Xu, and Y. Fang, "Blind image quality assessment using statistical structural and luminance features," *IEEE Transactions on Multimedia*, vol. 18, no. 12, pp. 2457–2469, 2016.

[9] Z. Wang, H. R. Sheikh, and A. C. Bovik, "No-reference perceptual quality assessment of jpeg compressed images," in *Proceedings. International Conference on Image Processing*, vol. 1. IEEE, 2002, pp. I–I.

[10] E. Ong, W. Lin, Z. Lu, X. Yang, S. Yao, F. Pan, L. Jiang, and F. Moschetti, "A no-reference quality metric for measuring image blur," in *Seventh International Symposium on Signal Processing and Its Applications, 2003. Proceedings.*, vol. 1. Ieee, 2003, pp. 469–472.

[11] Z. P. Sazzad, Y. Kawayoke, and Y. Horita, "No reference image quality assessment for jpeg2000 based on spatial features," *Signal Processing: Image Communication*, vol. 23, no. 4, pp. 257–268, 2008.

[12] Y. Fang, K. Ma, Z. Wang, W. Lin, Z. Fang, and G. Zhai, "No-reference quality assessment of contrast-distorted images based on natural scene statistics," *IEEE Signal Processing Letters*, vol. 22, no. 7, pp. 838–842, 2014.

[13] J. Chen, S. Shan, C. He, G. Zhao, M. Pietikainen, X. Chen, and W. Gao, "Wld: A robust local image descriptor," *IEEE transactions on pattern analysis and machine intelligence*, vol. 32, no. 9, pp. 1705–1720, 2009.

[14] B. Wang, W. Li, W. Yang, and Q. Liao, "Illumination normalization based on weber's law with application to face recognition," *IEEE Signal Processing Letters*, vol. 18, no. 8, pp. 462–465, 2011.

[15] X.-X. Li, L. He, P. Hao, Z. Liu, and J. Li, "Adaptive weberfaces for occlusion-robust face representation and recognition," *IET Image Processing*, vol. 11, no. 11, pp. 964–975, 2017.

[16] S. Bhattacharya, G. S. Nainala, S. Rooj, and A. Routray, "Local force pattern (lfp): Descriptor for heterogeneous face recognition," *Pattern Recognition Letters*, vol. 125, pp. 63–70, 2019.

[17] H. Roy and D. Bhattacharjee, "Local-gravity-face (lg-face) for illumination-invariant and heterogeneous face recognition," *IEEE Transactions on Information Forensics and Security*, vol. 11, no. 7, pp. 1412–1424, 2016.

[18] M. R. Faraji and X. Qi, "Face recognition under varying illuminations using logarithmic fractal dimension-based complete eight local directional patterns," *Neurocomputing*, vol. 199, pp. 16–30, 2016.

[19] S. Bhattacharya, A. Dasgupta, and A. Routray, "Robust face recognition of inferior quality images using local gabor phase quantization," in *2016 IEEE Students' Technology Symposium (TechSym)*. IEEE, 2017, pp. 294–298.

[20] Y. Gong, S. Lazebnik, A. Gordo, and F. Perronnin, "Iterative quantization: A procrustean approach to learning binary codes for large-scale image retrieval," *IEEE Transactions on Pattern Analysis and Machine Intelligence*, vol. 35, no. 12, pp. 2916–2929, 2012.

[21] A. K. Moorthy and A. C. Bovik, "Blind image quality assessment: From natural scene statistics to perceptual quality," *IEEE transactions on Image Processing*, vol. 20, no. 12, pp. 3350–3364, 2011.

[22] P. Ye, J. Kumar, L. Kang, and D. Doermann, "Unsupervised feature learning framework for no-reference image quality assessment," in *2012 IEEE conference on computer vision and pattern recognition*. IEEE, 2012, pp. 1098–1105.

[23] M. Minghui and Z. Chuanfeng, "Application of support vector machines to a small-sample prediction," *Advances in Petroleum Exploration and Development*, vol. 10, no. 2, pp. 72–75, 2015.

[24] "https://live.ece.utexas.edu/research/quality/subjective.htm."

[25] "http://vision.eng.shizuoka.ac.jp/mod/page/view.php?id=23."

[26] M. Zhang, C. Muramatsu, X. Zhou, T. Hara, and H. Fujita, "Blind image quality assessment using the joint statistics of generalized local binary pattern," *IEEE Signal Processing Letters*, vol. 22, no. 2, pp. 207–210, 2014.

[27] Z. Wang, A. C. Bovik, H. R. Sheikh, E. P. Simoncelli *et al.*, "Image quality assessment: from error visibility to structural similarity," *IEEE transactions on image processing*, vol. 13, no. 4, pp. 600–612, 2004.